MnxGa1−x nanodots with high coercivity and perpendicular magnetic anisotropy

Mn_xGa_{1-x} Nanodots with High Coercivity and Perpendicular Magnetic Anisotropy

J. Karel[1], F. Casoli[2], P. Lupo[2], F. Celegato[3], P. Tiberto[3], F. Albertini[2], C. Felser[1]

[1]Max-Planck-Institut für Chemische Physik fester Stoffe, Dresden, Germany 01187
[2]IMEM-CNR, Parma, Italy 43124
[3]INRIM, Electromagnetism Division, Turin, Italy 10135

Abstract

A Mn_xGa_{1-x} (x=0.70) epitaxial thin film with perpendicular magnetic anisotropy and a large coercivity (H_c = 1T) was patterned into nanodots using a self-assembly nanolithography procedure. Nanostructuring is achieved by self-assembly of polystyrene nanospheres, which are reduced in size and in turn act as a mask for film etching. This procedure introduced some chemical disorder, which resulted in a soft magnetic component in the magnetic hysteresis loops. However, chemical order was recovered after vacuum annealing at low temperature. The resulting nanodots retain the properties of the original film, i.e. magnetization oriented perpendicular to the particle and large coercivity. Our results suggest this lithography procedure could be a promising direction for preparing spin valve devices.

Metastable tetragonal $D0_{22}$ phase Mn-Ga (from Mn_2Ga to Mn_3Ga) shows unique properties, which can be exploited for numerous spintronic devices.[1] The material exhibits a low saturation magnetization, due to the ferrimagnetic alignment of Mn on two inequivalent sublattices in the structure, which can be tuned by changing the Mn content (i.e.100 kA/m for Mn_3Ga to 400 kA/m for Mn_2Ga).[2,3,4,5,6,7] Additionally, it has low Gilbert damping, high uniaxial magnetic anisotropy, a high magnetic Curie temperature and spin polarization.[2,3,4,5,8,9] This combination of properties makes the material potentially relevant for spin torque driven memories and devices, such as spin transfer torque MRAMs (STT-MRAMs) and spin transfer oscillators (STOs). In these applications, a ferromagnetic electrode with large perpendicular magnetic anisotropy (PMA), high spin polarization and low damping is desirable to simultaneously improve thermal stability and reduce writing/driving current.[10,11,12,13] Among the high PMA candidates for spin transfer (ST) devices, tetragonal Mn-Ga (i.e. Mn_2Ga and Mn_3Ga) has the lowest Gilbert damping constant.[12] The $D0_{22}$ phase in fact shows a uniaxial anisotropy constant of 1 MJ/m^3, not far from the value of $L1_0$-FePt but with an extraordinarily low Gilbert damping constant of 0.01. [12,14] Additionally, the moderate saturation magnetization of the Mn-Ga alloy in the $D0_{22}$ phase can be advantageous for high density MRAMs, where dipolar interactions between neighboring memory cell elements have to be avoided.

Both STT-MRAMs and STOs require nanostructuring of the material, and fabrication experiments have indeed been pursued in both $L1_0$-FePt and $D0_{22}$ Mn-Ga as well as cubic $L1_0$ Mn-Ga. However, challenges still remain. Annealing or growth temperatures of 450°C or higher are required to obtain nanodots of high PMA $L1_0$ phases,[14,15] and nanostructuring of $L1_0$ Mn-Ga required the use of electron beam lithography.[16] These procedures are not ideal for device fabrication. Moreover, nanofabrication of $L1_0$ or $D0_{22}$ Mn-Ga structures has resulted in multi-phase particles or particles with irregular shapes and sizes.[17,18,19] In this work, we show that thin films of Mn_xGa_{1-x} (x=0.70) exhibit PMA with coercivities up to 1 T, that the film can be easily patterned into nanodots with a diameter of 500 nm by self-assembly nanolithography and, finally, that the dots recover the magnetic properties of the film after low temperature annealing. This work is the first demonstration of the fabrication of $D0_{22}$ Mn-Ga nanodots.

An Mn_xGa_{1-x} thin film with x=0.70 (40nm) was prepared by RF sputtering from MnGa and Mn targets; the individual sputter rates were adjusted to obtain the desired composition. The film was prepared on an $SrTiO_3$ substrate at 300°C with a 5nm Pt capping layer deposited at room temperature to prevent oxidation. The nanostructuring was accomplished using a self-assembled nanolithography process including scanning electron microscopy (SEM). After the nanostructuring process, annealing treatments at temperatures below 200°C were utilized to improve the nanostructured sample properties. Characterization was performed using X-ray diffraction (XRD), SQUID magnetometry, atomic force microscopy (AFM) and magnetic force microscopy (MFM). Figure 1a shows the typical θ-2θ XRD pattern from the Mn_xGa_{1-x} film displaying the $D0_{22}$ structure with the c-axis oriented out of the plane of the film. The absence of mosaicity was confirmed by an azimuthal (ϕ) scan which shows the expected four-fold symmetry (Fig. 1b). Figure 1c shows magnetization (M) as a function of applied magnetic field (H) for

the unpatterned film with H applied parallel or perpendicular to the film plane, as indicated. The out of plane direction is the magnetic easy axis, exhibiting an M_s value of 225 emu/cm^3 and a coercivity of 1 T. The in-plane direction does not saturate up to 5 T. These results are consistent with previous reports.[7,8] Further details of the film characterization are presented elsewhere.[20]

This film was patterned using a self-assembled nanolithography process, which is shown in Figure 2.1-2.6. Each subfigure contains a schematic of the nanolithography step and an SEM image (when applicable). The film presents a maze-like morphology (Figure 2.1). The polystyrene nanospheres (800 nm) are combined with a solvent and deposited on the film by dip coating; the solvent evaporates, leaving the self-assembled nanospheres (Figure 2.2). These spheres are then reduced by plasma reduction to a size of 550-600 nm (Figure 2.3). Then the film is etched by sputter etching (Figure 2.4), and the spheres are removed (Figure 2.5), revealing the nanodots (Figure 2.6). The features in the nanodots reflect the morphology of the original film.

Figure 3a compares the normalized magnetization measured at room temperature for the film, nanodots and nanodots after annealing in vacuum below 200^{o}C for 6 hours; a kink near $H=0$ is evidenced in the curve of the nanostructured sample. This kink is significantly reduced after annealing the sample. Our previous work used transmission electron microscopy to show this secondary magnetic phase resulted from a fraction of the sample where the tetragonal c-axis was oriented in the film plane.[20] Other works have rather attributed this feature in the hysteresis loop to chemical disorder,[21] to interfacial canting or to alloying with seed layers resulting in superparamagnetic islands in the initial growth phase.[5, 22] In this work, the kink in the hysteresis loop of the nanostructured sample is likely due to chemical disorder induced during the sputter etching of the film. This conclusion is supported by XRD measurements shown in Figure 3b for the film, nanodots and nanodots after annealing. In the pattern for the nanodots before annealing, the 002 Mn_3Ga reflex which is a superlattice peak corresponding to a chemically ordered structure is absent. The peak is however present in the diffraction data measured on the film and nanodots after annealing, indicating that the etching process induces chemical disorder. Figures 3c, 3d show MFM images of the annealed nanodots in the demagnetized state and in a remnant state after application of H=7 T, respectively. The dots are magnetic and retain the perpendicular magnetic anisotropy of the original film. They are not single domain owing to the large size; the domain size of the dots is comparable to that of the original film.

In conclusion, a $Mn_{70}Ga_{30}$ epitaxial thin film was prepared and exhibited PMA and a large coercivity of approximately 1 T. A self-assembly nanolithography approach was used to pattern 550 nm nanostructures in the film. The resultant nanodots exhibited similar features to the parent film i.e. PMA and a large coercivity. A kink was evidenced in the magnetic hysteresis loop near H=0 in the nanostructured material and attributed to chemical disorder induced during the lithography procedure. Chemical order was recovered in the nanostructures after annealing at low temperatures. The nanodots exhibited multiple magnetic domains due to their size, and therefore a future research direction includes reducing the size of the nanostructures. Our results point to this

nanosphere lithography as a promising approach to effectively prepare magnetic nanostructures with the magnetization oriented perpendicular to the structure, making it potentially relevant for spintronic devices such as STT-MRAM and STOs.

Figure Captions

Figure 1. (a) θ-2θ XRD pattern, **(b)** azimuthal (ϕ) scan around the off-axis 112 peak and **(c)** in-plane (solid) and out-of-plane (dashed) magnetization at room temperature versus applied magnetic field for the Mn_xGa film (x=0.70). The grey squares (red squares) in (a) identify peaks from the substrate (Pt cap).

Figure 2. Schematic of nanolithography procedure and corresponding scanning electron microsope image. See text for detailed description.

Figure 3. (a) Normalized magnetic hysteresis loops measured at 300K and **(b)** θ-2θ XRD pattern of the 002 Mn_3Ga superlattice peak for the film, nanostructures and nanostructures after annealing. The grey box in (b) indicates the substrate peak. **(c-d)** MFM image of the nanodots after annealing. The images were taken after demagnetization from H= ±7T (c) and in a remnant state after application of H=7T (d).

References

[1] J. Winterlik, S. Chadov, A. Gupta, V. Alijani, T. Gasi, K. Filsinger, B. Balke, G.H. Fecher, C.A. Jenkins, F. Casper, J. Kueler, G.-D. Liu, L. Gao, S.S.P. Parkin, C. Felser, *Adv. Mater.* **24**, 6283 (2012)

[2] K. Rode, N. Baadji, D. Betto, Y.-C. Lau, H. Kurt, M. Venkatesan, P. Stamenov, S. Sanvito, J.M.D. Coey, E. Fonda, E. Otero, F. Choueikani, P. Ohresser, F. Porcher, G. Andre, *Phys. Rev. B.* **87** 184429 (2013)

[3] J. Winterlik, B. Balke, G.H. Fecher, C. Felser, M.C.M. Alves, F. Bernardi, J. Morais, *Phys Rev B* **77** 054406 (2008)

[4] B. Balke, G.H. Fecher, J. Winterlik, C. Felser, *Appl. Phys. Lett.* **90** 152504 (2007)

[5] M. Li, X. Jiang, M.G. Samant, C. Felser, S.S.P. Parkin, *Appl. Phys. Lett.* **103** 032410 (2013)

[6] S. Mizukami, T. Kubota, F. Wu, X. Zhang, T. Miyazaki, H. Naganuma, M. Oogane, A. Sakuma, Y. Ando, *Phys. Rev. B.* **85** 014416 (2012)

[7] J. Winterlik, S. Chadov, A. Gupta, V. Alijani, T. Gasi, K. Filsinger, B. Balke, G.H. Fecher, C.A. Jenkins, F. Casper, J. Kueler, G.-D. Liu, L. Gao, S.S.P. Parkin, C. Felser, *Adv. Mater.* **24**, 6283 (2012)

[8] H. Kurt, K. Rhode, M. Venkatesan, P. Stamenov, J.M.D. Coey, *Phys. Rev. B.* **83** 020405(R) (2011)

[9] H. Kurt, K. Rhode, M. Venkatesan, P. Stemenov, J.M.D. Coey, *Phys. Status Solidi B* **248** 2238 (2011)

[10] R.L. Stamps, S. Breitkreutz, J. Åkerman, A.V. Chumak, Y.C. Otani, G.E.W. Bauer, J.-U. Thiele, M. Bowen, S.A. Majetich, M. Kläui, I.L. Prejbeanu, B. Dieny, N.M. Dempsey, B. Hillebrands, *J. Phys. D: Appl. Phys.* **47** 333001 (2014)

[11] D. Houssameddine, U. Ebels, B. Delaët, B. Rodmacq, I. Firastrau, F. Ponthenier, M. Brunet, C. Thirion, J.P. Michel, L. Prejbeanu-Buda, M.-C. Cyrille, O. Redon, B. Dieny, *Nature Materials*, **6** 447 (2007)

[12] Q. Ma, A. Sugihara, K. Suzuki, X. Zhang, T. Miyazaki, T., S. Mizukami, *Spin* **04**, 1440024 (2014)

[13] A. D. Kent, D. C. Worledge. *Nature Nanotechnology* **10**, 187 (2015).

[14] Z.J. Yan, S. Takahashi, Y. Kondo, J. Ariake, T. Sakon, D.S. Xue, S. Ishio, *J. Phys. D-Appl. Phys.* **44** (2011) 185002.

[15] Z. Li, W. Zhang, K. M. Krishnan, *AIP Advances*, **5** 087165 (2015)

[16] D. Oshima, T. Kato, S. Iwata, S. Tsunashima, *IEEE Trans. Magn.* **49** 3608 (2013)

[17] T.J. Nummy, S.P. Bennett, T. Cardinal, D. Heiman, *Appl. Phys. Lett.* **99** 252506 (2011)

[18] C.L. Zha, R.K. Dumas, J.W. Lau, S.M. Mohseni, S. R. Sani, I.V. Golosovsky, A.F. Monsen, J. Nogues, J. Akerman, *J. Appl. Phys.* **110** 093902 (2011)

[19] C.L. Zha, R.K. Dumas, J.W. Lau, S.M. Mohseni, S.R. Sani, I.V. Golosovsky, A.F. Monsen, J. Nogues, J. Akerman, *J. Appl. Phys.* **110** 093902 (2011)

[20] J. Karel, F. Casoli, P. Lupo, L. Nasi, S. Fabbrici, L. Righi, F. Albertini, C. Felser, accepted *Scripta Materialia*

[21] L. Zhu, S. Nie, K. Meng, D. Pan J. Zhao, H. Zheng, *Adv. Mater.* **24** 4547 (2012)

[22] F. Wu, S. Mizukami, D. Watanabe, H. Nagunuma, M. Oogane, Y. Ando, T. Miyazaki, *Appl. Phys. Lett.* **94** 122503 (2009)

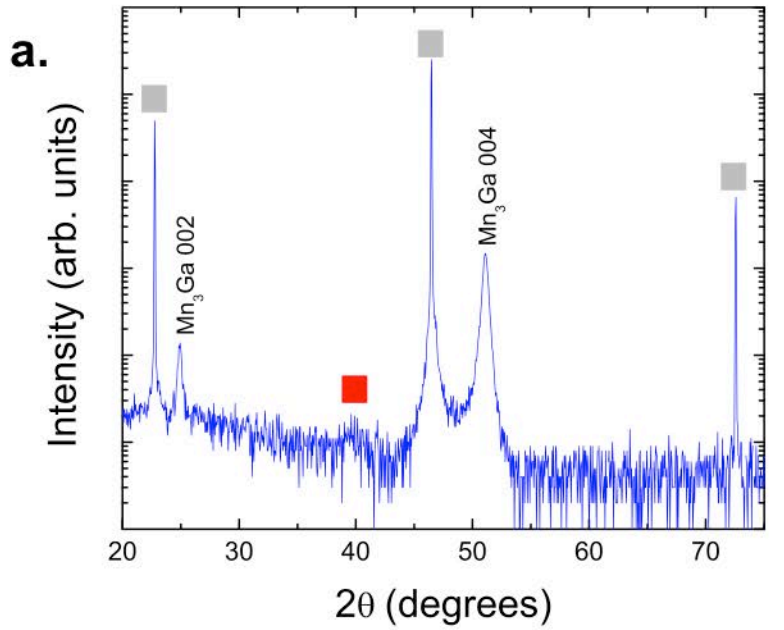
a.
Intensity (arb. units)
Mn3Ga 002
Mn3Ga 004
20
30
40
50
60
70
2θ (degrees)

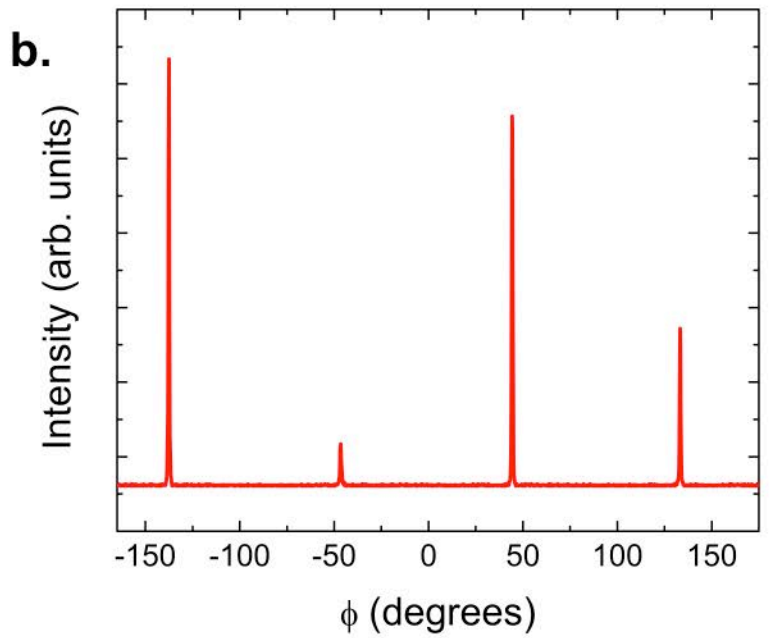
b.
Intensity (arb. units)
-150
-100
-50
0
50
100
150
ϕ (degrees)

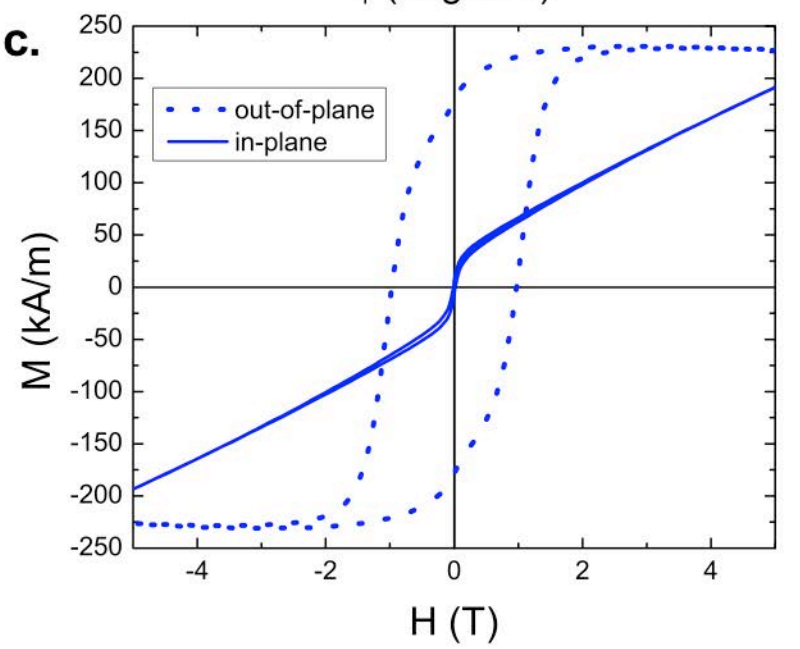
c.
out-of-plane
in-plane
M (kA/m)
250
200
150
100
50
0
-50
-100
-150
-200
-250
-4
-2
0
2
4
H (T)

1 Mn_xGa_{1-x} (x=0.70) film on STO substrate

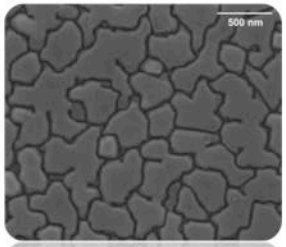

2 Polystyrene nanosphere (800 nm) deposition by floating technique

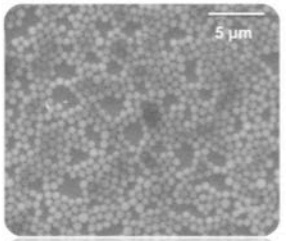

3 Nanosphere reduction to 600-550 nm by plasma reduction

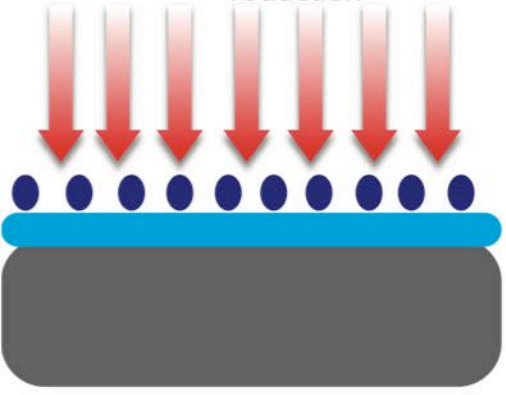

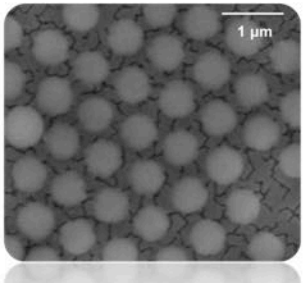

4 Mn_xGa_{1-x} film removal by sputter etching

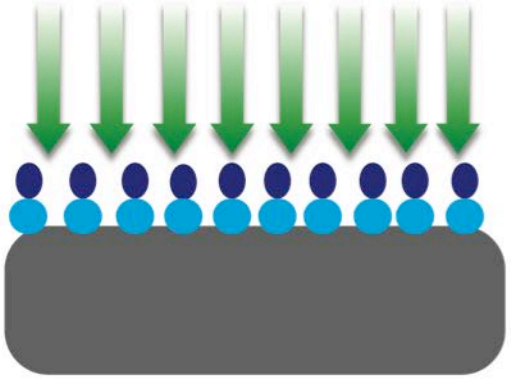

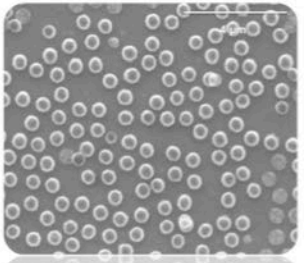

5 Nanosphere removal in ultrasonic bath with water solution

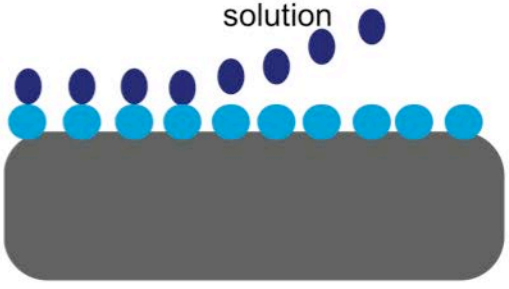

6 Mn_xGa_{1-x} nanodisks

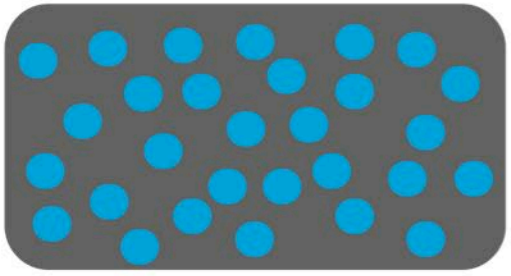

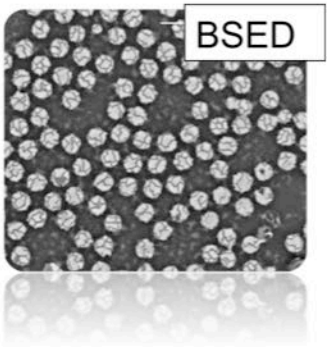

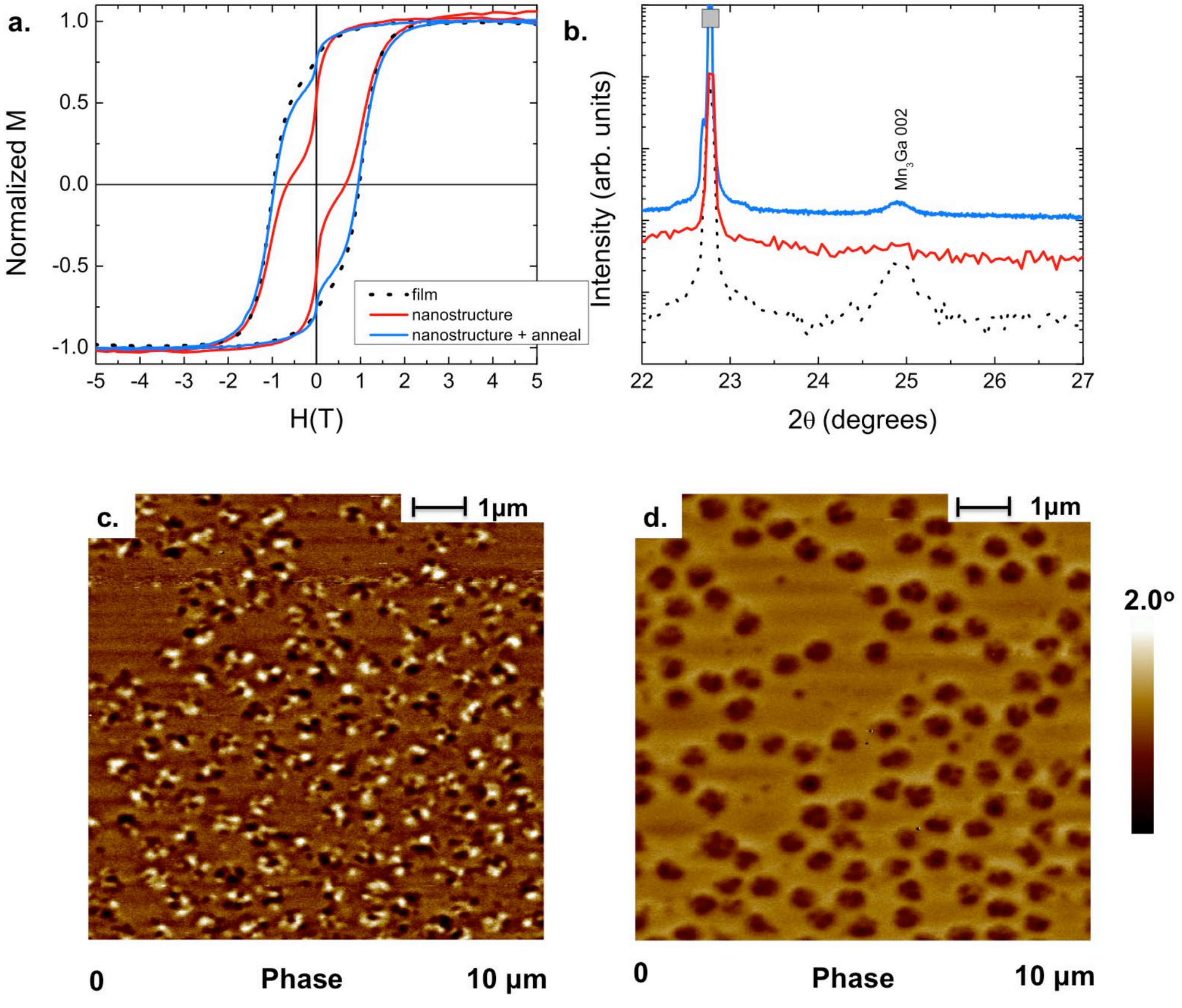
a.
Normalized M
H(T)
film
nanostructure
nanostructure + anneal
b.
Intensity (arb. units)
2θ (degrees)
Mn3Ga 002
c.
1μm
0
Phase
10 μm
d.
1μm
0
Phase
10 μm
2.0°